nature medicine

Induction of interleukin-8 preserves the angiogenic response in HIF-1α–deficient colon cancer cells

Yusuke Mizukami[1], Won-Seok Jo[1], Eva-Maria Duerr[1], Manish Gala[1], Jingnan Li[1], Xiaobo Zhang[1], Michael A Zimmer[2], Othon Iliopoulos[2], Lawrence R Zukerberg[3], Yutaka Kohgo[4], Maureen P Lynch[5], Bo R Rueda[5] & Daniel C Chung[1]

Hypoxia inducible factor-1 (HIF-1) is considered a crucial mediator of the cellular response to hypoxia through its regulation of genes that control angiogenesis[1–4]. It represents an attractive therapeutic target[5,6] in colon cancer, one of the few tumor types that shows a clinical response to antiangiogenic therapy[7]. But it is unclear whether inhibition of HIF-1 alone is sufficient to block tumor angiogenesis[8,9]. In HIF-1α knockdown DLD-1 colon cancer cells (DLD-1$^{HIF\text{-}kd}$), the hypoxic induction of vascular endothelial growth factor (VEGF) was only partially blocked. Xenografts remained highly vascularized with microvessel densities identical to DLD-1 tumors that had wild-type HIF-1α (DLD-1$^{HIF\text{-}wt}$). In addition to the preserved expression of VEGF, the proangiogenic cytokine interleukin (IL)-8 was induced by hypoxia in DLD-1$^{HIF\text{-}kd}$ but not DLD-1$^{HIF\text{-}wt}$ cells. This induction was mediated by the production of hydrogen peroxide and subsequent activation of NF-κB. Furthermore, the *KRAS* oncogene, which is commonly mutated in colon cancer, enhanced the hypoxic induction of IL-8. A neutralizing antibody to IL-8 substantially inhibited angiogenesis and tumor growth in DLD-1$^{HIF\text{-}kd}$ but not DLD-1$^{HIF\text{-}wt}$ xenografts, verifying the functional significance of this IL-8 response. Thus, compensatory pathways can be activated to preserve the tumor angiogenic response, and strategies that inhibit HIF-1α may be most effective when IL-8 is simultaneously targeted.

We subcutaneously injected DLD-1 cells, which contained either wild-type HIF-1α or HIF-1α stably knocked down by siRNA[10] (DLD-1$^{HIF\text{-}wt}$ or DLD-1$^{HIF\text{-}kd}$, respectively), into CD1 nude mice. Four weeks after inoculation, tumor volumes and weights were significantly lower in DLD-1$^{HIF\text{-}kd}$ tumors (**Fig. 1a**,**b**), indicating an important role for HIF-1 in tumor growth *in vivo*. We confirmed this finding in an independent colon cancer cell line, Caco2 (**Supplementary Fig. 1** online). Large necrotic areas were much more prevalent in DLD-1$^{HIF\text{-}wt}$ xenografts (**Fig. 1c**). Furthermore, a prominent inflammatory infiltrate composed predominantly of neutrophils was observed only in DLD-1$^{HIF\text{-}kd}$ xenografts (**Fig. 1c**). Although there were larger areas of necrosis in DLD-1$^{HIF\text{-}wt}$ xenografts, the cross-sectional surface area of non-necrotic viable tumor was still significantly greater when compared to DLD-1$^{HIF\text{-}kd}$ xenografts (0.33 cm^2 versus 0.16 cm^2, respectively, $P = 0.025$). Thus, the difference in size of the tumors cannot be entirely attributed to the larger area of necrosis in the DLD-1$^{HIF\text{-}wt}$ tumors. A persistent silencing effect of the HIF-1α siRNA construct was confirmed *in vivo* (**Fig. 1d**).

There was a significant decrease in the Ki-67 labeling index in DLD-1$^{HIF\text{-}kd}$ xenografts (41.3 ± 3.2% in DLD-1$^{HIF\text{-}wt}$ tumors versus 27.4 ± 2.6% in DLD-1$^{HIF\text{-}kd}$ tumors; $P < 0.01$), suggesting that HIF-1α regulates cellular proliferation *in vivo*. We calculated the apoptotic index by counting TUNEL-positive cells in non-necrotic areas. We observed a small but statistically significant difference in the apoptotic index between the two groups (3.2 ± 0.53% in DLD-1$^{HIF\text{-}wt}$ tumors versus 1.9 ± 0.42% in DLD-1$^{HIF\text{-}kd}$ tumors; $P < 0.05$), but this difference is unlikely to counterbalance the considerable difference in proliferation rates.

When we incubated DLD-1$^{HIF\text{-}kd}$ cells under hypoxic conditions (1% O_2) *in vitro*, we observed only a 25% reduction ($P = 0.11$) in the induced levels of *VEGF* mRNA and protein (**Fig. 1e**). In the DLD-1$^{HIF\text{-}kd}$ xenografts, *VEGF* mRNA and protein levels were also induced (**Fig. 1f**), though not to the same extent observed *in vitro*. Compared to the DLD-1$^{HIF\text{-}wt}$ xenografts, *VEGF* mRNA levels were 51% lower ($P = 0.028$) and protein levels were 52% lower ($P = 0.0024$) in DLD-1$^{HIF\text{-}kd}$ xenografts. This persistent expression of VEGF was not mediated by HIF-2α, as mRNA encoding HIF-2α and HIF-2α protein levels were barely detectable in normoxic conditions and the gene was not induced by hypoxia (**Supplementary Fig. 2** online).

To specifically address whether hypoxia regulates VEGF in the absence of HIF-1 *in vivo*, we identified hypoxic areas within the tumor mass using Hypoxyprobe-1 (pimonidazole hydroxychloride). There were large hypoxic regions surrounding the necrotic areas in the center of the DLD-1$^{HIF\text{-}wt}$ tumors (**Fig. 1g**). In contrast, DLD-1$^{HIF\text{-}kd}$ tumors showed only restricted regions of intratumoral hypoxia. Double immunofluorescence showed that VEGF was preferentially

[1]Gastrointestinal Unit, [2]Oncology Unit, Department of Medicine and [3]Department of Pathology, Massachusetts General Hospital and Harvard Medical School, 50 Blossom Street, Boston, Massachusetts 02114, USA. [4]Third Department of Internal Medicine, Asahikawa Medical College, 2-1 Midorigaoka-Higashi, Asahikawa, 078-8510 Japan. [5]Vincent Center for Reproductive Biology, Department of Obstetrics and Gynecology, Massachusetts General Hospital and Harvard Medical School, 50 Blossom Street Boston, Massachusetts 02114, USA. Correspondence should be addressed to D.C.C. (chung.daniel@mgh.harvard.edu).

Published online 28 August 2005; doi:10.1038/nm1294

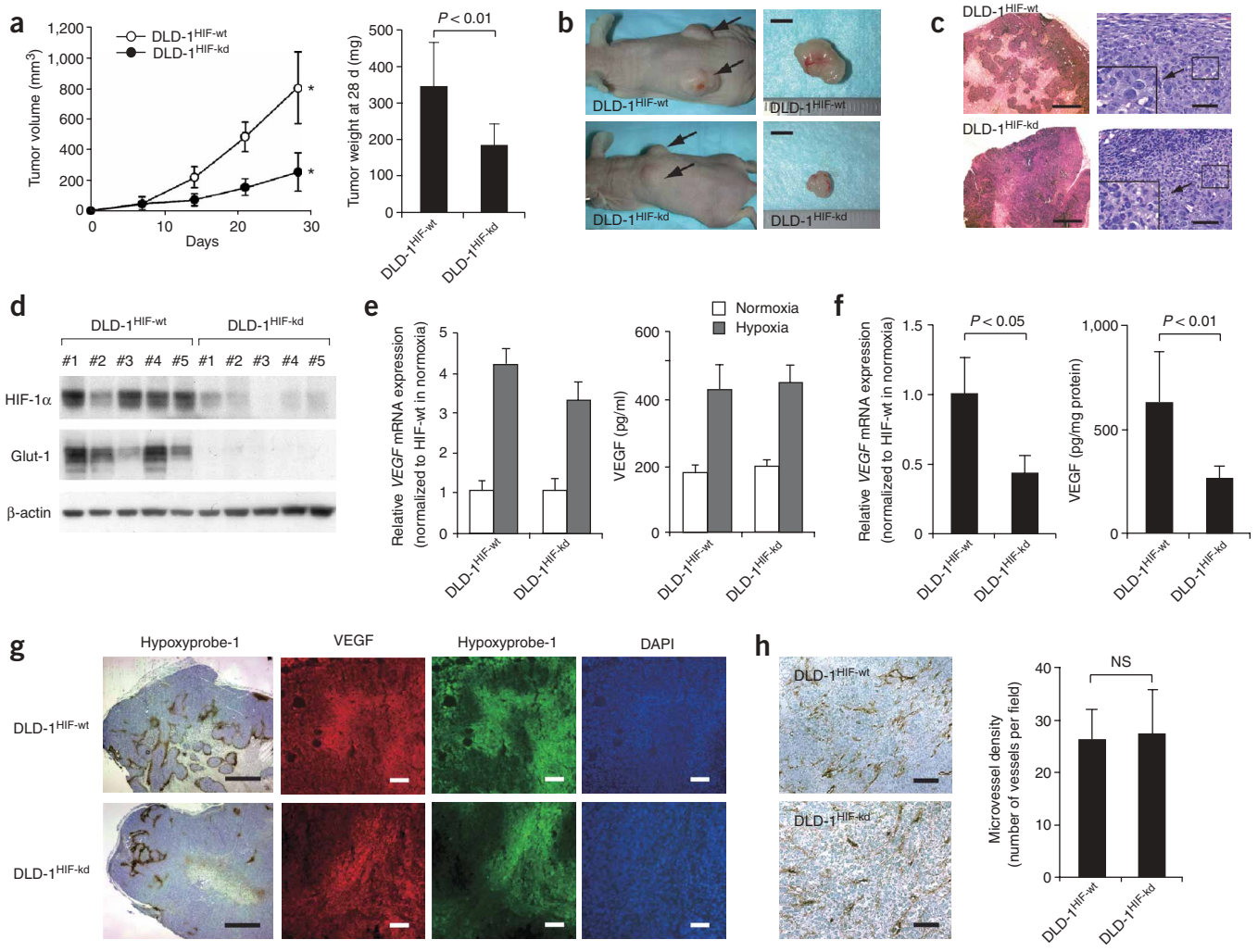

Figure 1 Growth of DLD-1$^{HIF\text{-}kd}$ cells *in vivo*. (**a**) Tumor volume and weight of DLD-1$^{HIF\text{-}wt}$ and DLD-1$^{HIF\text{-}kd}$ xenografts. *$P < 0.05$. (**b**) Gross appearance of xenografts and excised tumors at 4 weeks. Scale bar, 5 mm. (**c**) H&E staining of resected tumors. Left scale bars, 1 mm; right scale bars, 50 μm. (**d**) Immunoblotting for HIF-1α and Glut-1 in DLD-1$^{HIF\text{-}kd}$ xenografts. *VEGF* mRNA and protein levels in cultured DLD-1 cells (**e**) and in tumor xenografts (**f**) were measured. (**g**) Intratumoral 'hypoxia' was detected by immunohistochemistry for Hypoxyprobe-1. Scale bar, 1 mm. Immunofluorescent staining for VEGF (Texas red) and Hypoxyprobe-1 (FITC). Scale bar, 100 μm. (**h**) Immunohistochemistry for CD31 and quantification of microvessel density in DLD-1 xenografts. Scale bar, 100 μm.

expressed in the hypoxic areas of both DLD-1$^{HIF\text{-}kd}$ and DLD-1$^{HIF\text{-}wt}$ xenografts (**Fig. 1g**).

It is possible that the difference in growth between the xenografts resulted from impaired angiogenesis, potentially attributable to lower levels of VEGF in DLD-1$^{HIF\text{-}kd}$ tumors. But immunostaining for the endothelial cell marker CD31 showed abundant microvascular networks in all tumors (**Fig. 1h**). We observed no quantitative difference in microvessel density (26.1 ± 6.3/field in DLD-1$^{HIF\text{-}wt}$ and 28.7 ± 8.6/field in DLD-1$^{HIF\text{-}kd}$ xenografts), suggesting that high levels of HIF-1 may not be required to stimulate angiogenesis or maintain vessel integrity in DLD-1 tumors.

Although upregulation of VEGF was preserved in DLD-1$^{HIF\text{-}kd}$ xenografts, the absolute levels of VEGF were reduced. We therefore determined whether other angiogenic factors may be induced in a compensatory manner to maintain tumor vascularity in the absence of HIF-1. cDNA microarray analysis identified genes that were upregulated at least twofold by hypoxia but whose expression was attenuated less than 30% when HIF-1 was silenced. *VEGF* was upregulated fourfold in DLD-1$^{HIF\text{-}wt}$ cells by hypoxia, and this induction was decreased only 10.6% by HIF-1 silencing (**Supplementary Table 1** online). In addition, expression of the proangiogenic cytokine *IL-8* was increased twofold in DLD-1$^{HIF\text{-}kd}$ cells cultured in hypoxic conditions compared to DLD-1$^{HIF\text{-}wt}$ cells.

Hypoxia upregulated *IL-8* mRNA >2.5-fold in DLD-1$^{HIF\text{-}kd}$ cells, but there was no induction in DLD-1$^{HIF\text{-}wt}$ cells (**Fig. 2a**). Consistent with this result, the level of IL-8 in the supernatant of DLD-1$^{HIF\text{-}kd}$ cells was increased almost threefold compared to DLD-1$^{HIF\text{-}wt}$ cells. We obtained similar results with previously established, independent DLD-1$^{HIF\text{-}kd}$ clones[10] (data not shown). Extracts from DLD-1$^{HIF\text{-}kd}$ xenografts also showed significantly higher *IL8* mRNA and protein levels when compared to DLD-1$^{HIF\text{-}wt}$ tumors (**Fig. 2b**). *IL-8* promoter reporter constructs showed higher basal activity in DLD-1$^{HIF\text{-}kd}$ cells (**Fig. 2c**), and there was further induction of promoter activity in hypoxia that was not observed in the DLD-1$^{HIF\text{-}wt}$ cells. There was also a 2.1-fold induction of the *IL-8* promoter when HIF-1α was transiently knocked down in parental DLD-1 cells, indicating this

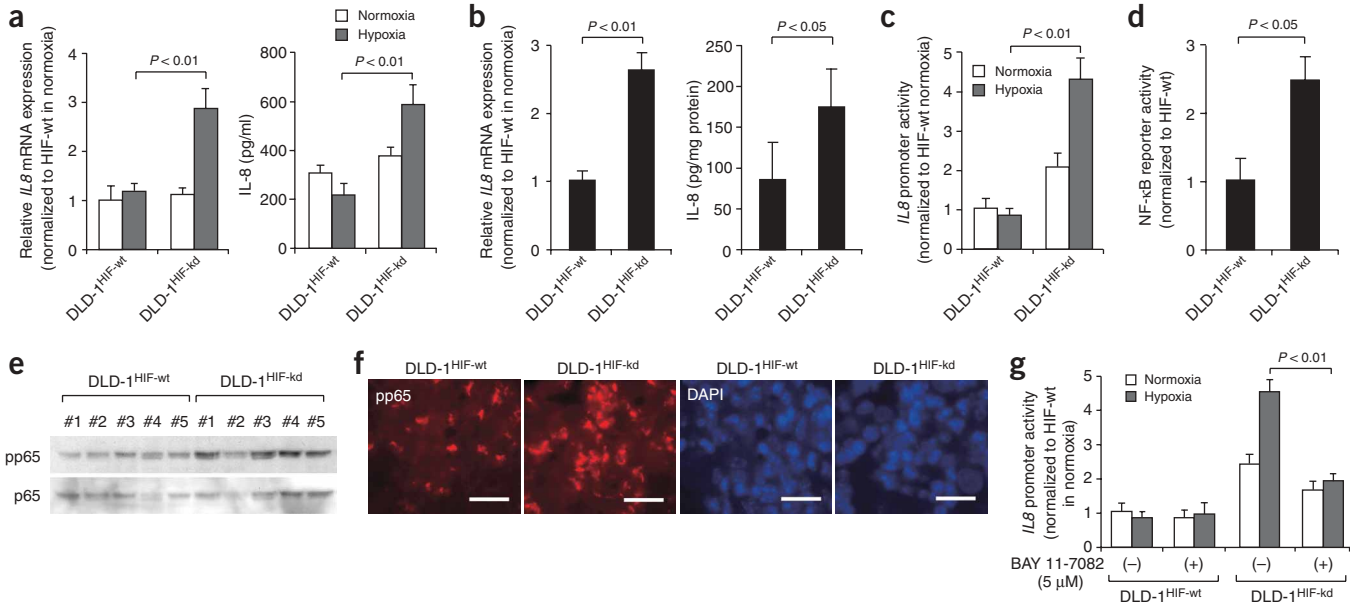

Figure 2 Knockdown of HIF-1 facilitates the induction of IL-8 by NF-κB during hypoxic conditions. *IL8* mRNA and protein levels in (**a**) cultured DLD-1 cells and (**b**) DLD-1 xenografts. (**c**) *IL8* promoter activity during hypoxia in DLD-1$^{HIF\text{-}kd}$ and DLD-1$^{HIF\text{-}wt}$ cells. (**d**) NF-κB reporter activity in hypoxic conditions in DLD-1$^{HIF\text{-}kd}$ cells. (**e**) Immunoblotting for NF-κB, p65 subunit and Ser536-phosphorylated p65 (p-p65), in DLD-1 tumor lysates. (**f**) Immunohistochemistry for phosphorylated p65 in DLD-1 xenografts (shown as Texas Red). Scale bar, 50 μm. (**g**) Effect of NF-κB inhibition on *IL8* promoter activity with BAY 11-7082.

phenomenon was not an artifact of the stable transfection process. In addition, expression of a constitutively active HIF-1α in which the proline at position 564 was changed to an alanine in DLD-1 cells did not induce the *IL-8* promoter (1.01 ± 0.14-fold increase), indicating that HIF-1 does not directly regulate *IL-8* gene expression. This hypoxic effect was not unique to DLD-1 cells. Knockdown of HIF-1α in additional colon cancer cells (ColoHSR, SW 480 and HCT116), pancreatic cancer cells (Panc-1, CAPAN-1), breast cancer cells (MDA-MB-453) and lung cancer cells (HOP-92) showed a similar induction of IL-8 in hypoxia (**Supplementary Fig. 3** online). Finally, we confirmed specificity of these siRNA constructs by observing expression of HIF-1α synonymous codon mutants (**Supplementary Fig. 4** online). The absence of HIF-1 can therefore stimulate IL-8 on a transcriptional level, and this is further enhanced in hypoxia.

NF-κB is a major regulator of IL-8. NF-κB reporter activity was increased 151% ($P < 0.01$) in HIF-1α knockdown cells (**Fig. 2d**). Western blotting (**Fig. 2e**) and immunohistochemistry (**Fig. 2f**) of tissue xenografts showed that phosphorylation of the p65 subunit was greater in DLD-1$^{HIF\text{-}kd}$ xenografts, suggesting that HIF-1 inhibition does upregulate the NF-κB pathway *in vivo*. Densitometry of western blots quantified a 2.0 ± 0.4-fold increase in the ratio of phosphorylated p65 to unphosphorylated p65 ($P < 0.01$). The hypoxic induction of the *IL-8* promoter in DLD-1$^{HIF\text{-}kd}$ cells was significantly downregulated by BAY 11-7082, a specific inhibitor of NF-κB[11] (**Fig. 2g**). Thus, activation of the NF-κB pathway is important for the induction of IL-8 in the absence of HIF-1.

We then speculated that HIF-1 inhibition may enhance the production of hydrogen peroxide (H_2O_2), a reactive oxygen species (ROS) that can activate NF-κB[12,13]. Hypoxic conditions can lead to the increased production of ROS[14,15], and scavenging of ROS is often achieved by increased production of pyruvate[16] that occurs when cells shift from oxidative to glycolytic metabolism. This shift depends upon HIF-1α[17]. DLD-1$^{HIF\text{-}kd}$ cells released more H_2O_2 *in vitro*, and hypoxia further enhanced its production (**Fig. 3a**). Four distinct chemical inhibitors of ROS production (*N*-acetyl-L-cysteine, pyrrolidinedithiocarbamate, rotenone and diphenylene iodonium) each strongly blocked the induction of NF-κB promoter activity by hypoxia in DLD-1$^{HIF\text{-}kd}$ cells (**Fig. 3b**). Finally, exogenous administration of the long-acting H_2O_2 analog, *t*-butyl hydroperoxide, stimulated the production of IL-8 in parental DLD-1 cells. This induction was inhibited by BAY 11-7082 (**Fig. 3c**), again showing that NF-κB mediates this effect of ROS.

In contrast to DLD-1$^{HIF\text{-}kd}$ cells, we did not observe hypoxic induction of *IL8* mRNA (**Fig. 3d**) and protein (data not shown) in Caco2$^{HIF\text{-}kd}$ colon cancer cells[10]. Given that DLD-1 cells harbor the Gly13Asp mutation in the *KRAS* oncogene (*KRAS*38g→a), whereas Caco2 cells are wild-type (*KRAS*$^{35g/35g}$), we speculated that oncogenic *KRAS* may have a role in the hypoxic induction of IL-8 (ref. 18). When we induced the expression of the Gly12Val *KRAS* mutation (KRAS35g→t) in Caco2$^{HIF\text{-}kd}$ cells , hypoxia upregulated *IL-8* mRNA 2.5-fold, whereas the effect was not observed in Caco2$^{HIF\text{-}wt}$ cells or in Caco2$^{HIF\text{-}kd}$ cells exposed to hypoxia only (**Fig. 3d**). *KRAS*^{35t} only modestly induced *IL-8* mRNA in Caco2$^{HIF\text{-}kd}$ cells in normoxic conditions. Expression of *KRAS*^{35t} in Caco2$^{HIF\text{-}wt}$ cells also upregulated the *IL-8* promoter, but this activation was more pronounced in Caco2$^{HIF\text{-}kd}$ cells under conditions of hypoxia (**Fig. 3e**). BAY 11-7082 blocked the induction of the *IL-8* promoter by hypoxia and *KRAS*^{35t} (**Fig. 3e**).

Exogenous expression of oncogenic *KRAS* may act supraphysiologically. Endogenous *KRAS*^{38a} in DLD-1 cells was therefore silenced by siRNA and this resulted in a 50% reduction of KRAS protein levels, consistent with a silencing effect of the one mutant allele[19]. Knockdown of *KRAS*^{38a} attenuated the hypoxic induction of an NF-κB reporter and *IL8* promoter activity (**Fig. 3f**) as well as *IL8* mRNA levels (**Fig. 3g**) in DLD-1$^{HIF\text{-}kd}$ but not in DLD-1$^{HIF\text{-}wt}$ cells. These observations were confirmed in the Panc-1 pancreatic and PC3 prostate cancer cell lines, indicating the broader importance of *KRAS* on this alternative regulation of IL-8 (**Supplementary Fig. 5**

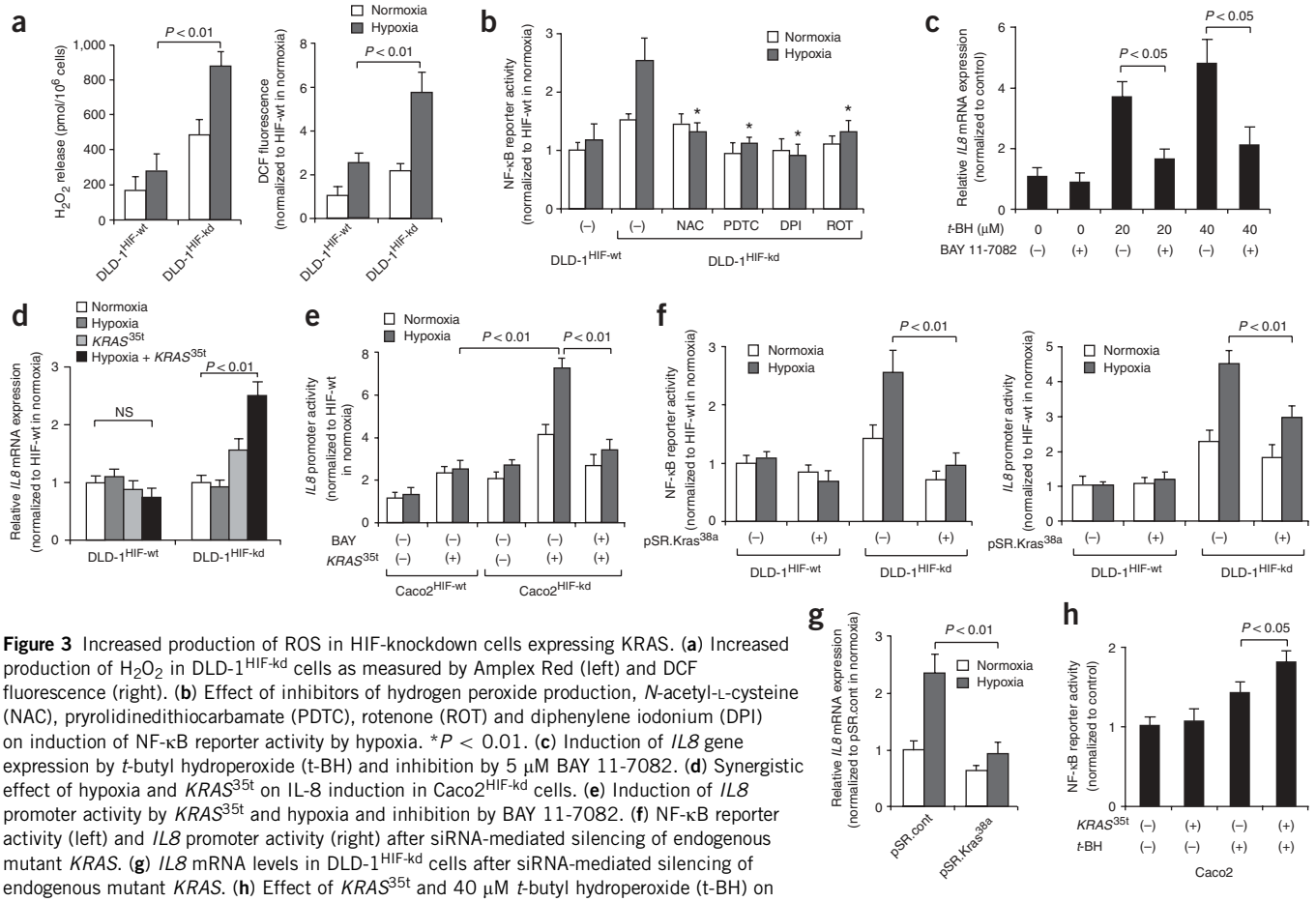

Figure 3 Increased production of ROS in HIF-knockdown cells expressing KRAS. (**a**) Increased production of H_2O_2 in DLD-$1^{HIF\text{-}kd}$ cells as measured by Amplex Red (left) and DCF fluorescence (right). (**b**) Effect of inhibitors of hydrogen peroxide production, *N*-acetyl-L-cysteine (NAC), pyrolidinedithiocarbamate (PDTC), rotenone (ROT) and diphenylene iodonium (DPI) on induction of NF-κB reporter activity by hypoxia. $^*P < 0.01$. (**c**) Induction of *IL8* gene expression by *t*-butyl hydroperoxide (t-BH) and inhibition by 5 μM BAY 11-7082. (**d**) Synergistic effect of hypoxia and $KRAS^{35t}$ on IL-8 induction in Caco$2^{HIF\text{-}kd}$ cells. (**e**) Induction of *IL8* promoter activity by $KRAS^{35t}$ and hypoxia and inhibition by BAY 11-7082. (**f**) NF-κB reporter activity (left) and *IL8* promoter activity (right) after siRNA-mediated silencing of endogenous mutant *KRAS*. (**g**) *IL8* mRNA levels in DLD-$1^{HIF\text{-}kd}$ cells after siRNA-mediated silencing of endogenous mutant *KRAS*. (**h**) Effect of $KRAS^{35t}$ and 40 μM *t*-butyl hydroperoxide (t-BH) on NF-κB reporter activity in Caco2 cells.

online). Furthermore, we observed the stimulatory effect of oncogenic *KRAS* on NF-κB in hypoxic conditions or in the presence of ROS (**Figs. 3d**,**h**). Collectively, these studies indicate that IL-8 can be induced in hypoxia through the activation of NF-κB in the absence of HIF-1, and that oncogenic *KRAS* can further stimulate NF-κB in hypoxic conditions to upregulate this alternative angiogenic pathway.

Finally, we sought to determine the functional significance of IL-8 production in HIF-1–deficient tumors. The observation that DLD-$1^{HIF\text{-}kd}$ xenografts showed a marked inflammatory infiltrate (**Fig. 1c**) was consistent with a functional role for IL-8, a potent neutrophil chemokine[18]. Intraperitoneal administration of the IL-8 neutralizing antibody MAB208 resulted in complete regression of 25% of DLD-$1^{HIF\text{-}kd}$ xenografts, and among the other detectable DLD-$1^{HIF\text{-}kd}$ tumors, there was a 61.3% reduction in tumor volume ($P < 0.01$) and 61.8% reduction in tumor weight ($P < 0.01$) compared to tumors treated with control IgG (**Fig. 4a**,**b**). In contrast, there was only a 24.8% ($P = 0.28$) and 15.6% ($P = 0.35$) reduction in tumor volume and weight, respectively, in DLD-$1^{HIF\text{-}wt}$ xenografts. Although treatment with MAB208 resulted in a decrease in the Ki-67 labeling index and increase in apoptosis in the DLD-$1^{HIF\text{-}kd}$ xenografts (**Fig. 4c**), *in vitro* studies showed that MAB208 did not directly inhibit tumor cell growth (**Fig. 4d**). Rather, treatment with MAB208 resulted in a considerable inhibition of angiogenesis. The microvessel density in DLD-$1^{HIF\text{-}kd}$ xenografts was reduced 46.5% ($P < 0.001$) compared to a 14.5% reduction ($P = 0.11$) in DLD-$1^{HIF\text{-}wt}$ xenografts (**Fig. 4e**). Confocal microscopy of tumor sections after lectin perfusion verified that vascular integrity was compromised in DLD-$1^{HIF\text{-}kd}$ xenografts treated with MAB208 (**Fig. 4e**). In addition to reduced vessel number, the vessels were markedly narrowed and fragmented. Specifically, the mean vessel diameter fell from 22.4 μm to 5.9 μm ($P = 0.0002$) when we treated DLD-$1^{HIF\text{-}kd}$ xenografts with MAB208, but there was no change in the DLD-$1^{HIF\text{-}wt}$ xenografts (26.5 μm versus 24.8 μm with MAB208; not significant). Neutralization of both IL-8 and VEGF in DLD-$1^{HIF\text{-}kd}$ xenografts had an additive effect on the inhibition of tumor growth (**Fig. 4f**), showing that each factor can regulate tumorigenesis independently.

In summary, we have shown that HIF-1α deficiency in colon cancer cells can inhibit proliferation and overall growth, but not angiogenesis. There are conflicting reports of the role of HIF-1 in tumor cell proliferation. *Hif1a*$^{-/-}$ embryonic stem cell–derived teratocarcinomas show reduced as well as increased growth[2,20]. Among human tumors, overexpression of HIF-1α has been associated with improved survival in individuals with head and neck cancers[21] and HIF-1 can inhibit the growth of renal carcinoma cells[22]. This may be mediated through the induction of the cell-cycle inhibitors p21 and p27 (ref. 23). It has been speculated that HIF-1 may have intrinsic functions to either promote or inhibit tumor growth that depends upon the cellular context[24]. The preservation of angiogenesis in our model can be explained by persistent expression of VEGF as well as induction of the proangiogenic factor, IL-8. IL-8 was stimulated by ROS-mediated activation of NF-κB, and this was enhanced by oncogenic *KRAS*. Neutralization of IL-8 in HIF-1–deficient tumors led to a substantial inhibition of

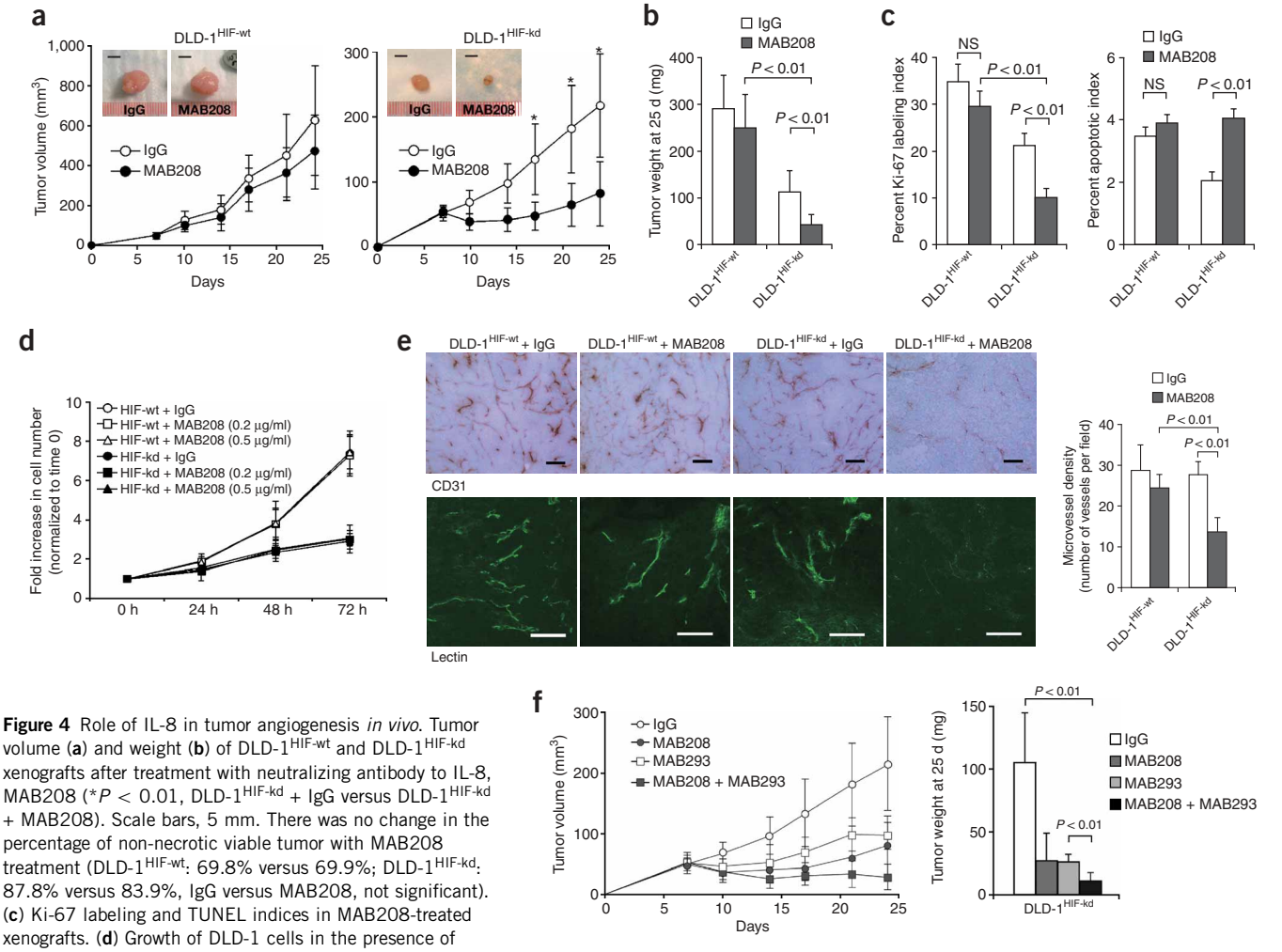

Figure 4 Role of IL-8 in tumor angiogenesis *in vivo*. Tumor volume (**a**) and weight (**b**) of DLD-1$^{HIF\text{-}wt}$ and DLD-1$^{HIF\text{-}kd}$ xenografts after treatment with neutralizing antibody to IL-8, MAB208 (*$P < 0.01$, DLD-1$^{HIF\text{-}kd}$ + IgG versus DLD-1$^{HIF\text{-}kd}$ + MAB208). Scale bars, 5 mm. There was no change in the percentage of non-necrotic viable tumor with MAB208 treatment (DLD-1$^{HIF\text{-}wt}$: 69.8% versus 69.9%; DLD-1$^{HIF\text{-}kd}$: 87.8% versus 83.9%, IgG versus MAB208, not significant). (**c**) Ki-67 labeling and TUNEL indices in MAB208-treated xenografts. (**d**) Growth of DLD-1 cells in the presence of MAB208 under hypoxic conditions. (**e**) Blood vessels visualized by CD31 immunohistochemistry (upper; scale bar, 100 μm) and lectin perfusion (lower; scale bar, 50 μm). Narrow and fragmented vessels are present in DLD-1$^{HIF\text{-}kd}$ + MAB208. (**f**) Growth of DLD-1$^{HIF\text{-}kd}$ xenografts when treated with a neutralizing VEGF antibody (MAB293) and/or a neutralizing antibody to IL-8 (MAB208). In these xenografts, the percentage of viable non-necrotic tumor fell slightly to 74.7% from 87.8% in mice that received control antibody only ($P = 0.1$).

angiogenesis and tumor growth. Studies of lung cancer cells harboring a *KRAS* mutation have also shown a pivotal role for IL-8 in tumor angiogenesis[25]. Collectively, these findings highlight the complex role of HIF-1α in colorectal tumorigenesis, the diversity of pathways used by tumors to stimulate angiogenesis, and the potential for combination antiangiogenic regimens that target both HIF-1 and IL-8.

METHODS

Cell lines. We stably transfected DLD-1 and Caco2 cells (ATCC) with HIF-1α–specific siRNA constructs (pSuper.retro, OligoEngine), pSR.HIF-1α1470 or pSR.HIF-1α2192 (ref. 10). Three independent DLD-1 clones stably expressing pSR.HIF-1α1470 and two independent clones expressing pSR.HIF-1α2192 showed similar responses to hypoxia with respect to induction of NF-κB and IL-8. In a pilot xenograft study, growth, microvascular density, VEGF and IL-8 levels were similar between a pSR.HIF-1α1470 clone and pSR.HIF-1α2192 clone. Hypoxic conditions (1% O_2) were achieved with a sealed hypoxia chamber (Billups-Rothenberg) in serum-free UltraCulture medium (Cambrex)[10]. We performed transient transfections using Lipofectamine 2000 (Invitrogen).

Plasmid constructs. The IL-8 reporter[26], NF-κB reporter and phr-GFP-KRAS^{35t} plasmids have been described[27]. We performed site-directed mutagenesis to obtain the phr-GFP-KRAS^{38a} construct. We constructed pSuper.Kras^{38a} (pSR.Kras^{38a}) by subcloning the sequence 5′-GGAGCTGGTGACGTAGGCA-3′. For control siRNA, pSR.cont, we used the sequence 5′-GCGCGCTTTGTAG GATTCG-3′ (ref. 28). For mutations in *KRAS*, we used a numbering system in which position 1 is the A of the initiator ATG codon. *KRAS*^{38a} results in a Gly13Asp mutation and *KRAS*^{35t} results in a Gly12Val mutation.

Transfections and reporter assays. We cotransfected 0.1–0.2 μg of reporter constructs with 2 ng of pRL-CMV (Promega) and measured luciferase activity with the Dual Luciferase Reporter Assay System (Promega). We used pRL-null, a promoter-less *Renilla* construct, when we cotransfected cells with a KRAS expression vector[29]. We calculated the relative luciferase activity as the ratio of firefly/*Renilla* luciferase activity. The level of 'hypoxic induction' was the ratio between the relative luciferase activity in hypoxia to that in normoxia.

Xenograft tumor model. We injected 2 × 10^6 cells subcutaneously into the flanks of 6–8-week-old CD1 female nude mice (six mice per arm). We measured tumors with calipers and calculated volume as (length × width^2) × 0.5. We intraperitoneally administered neutralizing antibody to IL-8 (MAB208, clone 6217.111; R&D Systems) and/or VEGF (MAB293, R&D Systems) when tumors reached 5 mm. We injected 100 μg of MAB208 and/or 25 μg of MAB293 on days 7, 9, 11, 14, 16, 18, 21 and 23, before mice were

killed at day 25. To assess hypoxic regions, we intraperitoneally injected mice with 60 mg/kg pimonidazol hydrochloride (Hypoxyprobe-1, Chemicon), 1.5 h before killing. To visualize functional tumor microvessels, we intravenously injected 100 μg FITC-labeled tomato lectin (Vector Laboratories), and perfused the hearts of the mice with 4% paraformaldehyde. This protocol was approved by the Animal Care and Use Committee of the Massachusetts General Hospital.

Immunohistochemistry. We treated 5-μm sections from fresh frozen tumors with acetone and blocked endogenous peroxidase with 3% H_2O_2. We incubated the sections with a CD31-specific antibody, MEC13.3 (1:50; Pharmingen), overnight at 4 °C. We counted blood vessels in 5–10 random viable fields (magnification, ×200). To detect tumor hypoxia, we treated formalin-fixed sections with 0.01% pronase and incubated them with Hypoxpyrobe-1–specific antibody Mab1 (1:50; Chemicon). For other immunohistochemical studies, we fixed xenograft tissues in 10% neutral buffered formalin. We performed TUNEL staining with the ApoAlert DNA fragmentation detection kit (Clontech). We performed Ki-67 staining with the MIB-1 antibody (1:100; DAKO) and performed staining for Ser563-phosphorylated p65 (1:50; Cell Signaling).

Real-time PCR assay. We extracted RNA using the RNeasy kit (Qiagen) and performed quantitative reverse transcription PCR using the SuperScript III platinum Two-Step qRT-PCR Kit (Invitrogen). Primer sequences for *VEGF*, *IL8* and 18S RNA are available upon request. We used a fluorogenic SYBR Green and MJ research detection system for real-time quantification.

Immunoblotting. We performed immunoblot analysis for HIF-1α (clone 54, 1:250; Transduction Laboratories), HIF-2α (1:250, Novus), Glut-1 (GT-11A, 1:1000; Alpha Diagnostic International), VEGF (Ab-2, 1:40; Calbiochem), Ser563-phosphorylated p65 and total NF-κB p65 (1:1,000; both Cell Signaling), KRAS (F234, 1:200; Santa Cruz) and β-actin (AC15, 1 μg/ml; Sigma) after SDS-PAGE and electrophoretic transfer to polyvinylidene fluoride membranes[10].

ELISA. We assayed the levels of VEGF and IL-8 protein in conditioned medium and tissue lysates using specific ELISA kits (Quantikine, R&D Systems).

Microarray analysis. We performed sample preparation and processing procedures as described in the Affymetrix GeneChip Expression Analysis Manual. We hybridized the labeled cRNA samples to the complete Affymetrix human U133 GeneChip set (HG-U133A).

Hydrogen peroxide studies. We measured H_2O_2 using the Amplex Red Hydrogen peroxide Assay Kit and the CM-H2DCFDA reagent (both from Molecular Probes). We exposed cells to hypoxia for 10 h, and then switched culture medium to Krebs-Ringer phosphate buffer[30] containing 100 μM Amplex Red reagent and 0.2 U/ml horseradish peroxidase. After additional incubation in hypoxia for 1 h, we measured fluorescence in 96-well plates using Spectra MAX GEMINI XS microplate fluorometer (Molecular Devices). We also incubated cells with 10 μM CM-H2DCFDA for 30 min in RPMI without phenol red. We measured fluorescence in 96-well plates and normalized values to cell number. We added 20 or 40 μM *t*-butyl hydroperoxide (Sigma) to the culture media of DLD-1 cells every 30 min for 6 h and measured *IL8* mRNA using qRT-PCR.

Statistical analysis. We performed statistical analyses with a two-tailed, unpaired Student *t*-test.

Note: Supplementary information is available on the Nature Medicine website.

ACKNOWLEDGMENTS

We thank the following individuals for sharing these plasmids: C. Reinecker (IL-8 reporter construct), R. Xavier (NF-κB reporter construct, phr-GFP-K-ras^{Val12}) and D. Tenen (pRL-null). We also thank Y. Kamegaya, M. Takeda, M. Ii, E. di Tomaso, T. Padera, P. Au and R. Tyszkowski for assistance with tissue analysis. DNA microarray studies were performed at the DNA Microarray Core Facility at the Massachusetts General Hospital Cancer Center. Confocal microscopy was performed through the Imaging Core of the Center for Study of Inflammatory Bowel Diseases. This work was supported by US National Institutes of Health (NIH) research grant CA92594 to D.C.C. O.I. was supported by NIH grant CA104574, B.R.R. was supported by NIH grant CA098333, M.A.Z. was supported by von Hippel-Lindau Family Alliance, M.G. was supported by an American Gastroenterology Association student fellowship award, and E.-M.D. was supported by a postdoctoral fellowship award from the Deutsche Forschungsgemeinschaft.

COMPETING INTERESTS STATEMENT

The authors declare that they have no competing financial interests.

Received 10 June; accepted 2 August 2005
Published online at http://www.nature.com/naturemedicine/

1. Denko, N.C. *et al.* Investigating hypoxic tumor physiology through gene expression patterns. *Oncogene* **22**, 5907–5914 (2003).
2. Carmeliet, P. *et al.* Role of HIF-1alpha in hypoxia-mediated apoptosis, cell proliferation and tumour angiogenesis. *Nature* **394**, 485–490 (1998).
3. Pugh, C.W. & Ratcliffe, P.J. Regulation of angiogenesis by hypoxia: role of the HIF system. *Nat. Med.* **9**, 677–684 (2003).
4. Tang, N. *et al.* Loss of HIF-1alpha in endothelial cells disrupts a hypoxia-driven VEGF autocrine loop necessary for tumorigenesis. *Cancer Cell* **6**, 485–495 (2004).
5. Kung, A.L., Wang, S., Klco, J.M., Kaelin, W.G. & Livingston, D.M. Suppression of tumor growth through disruption of hypoxia-inducible transcription. *Nat. Med.* **6**, 1335–1340 (2000).
6. Semenza, G.L. Targeting HIF-1 for cancer therapy. *Nat. Rev. Cancer* **3**, 721–732 (2003).
7. Hurwitz, H. *et al.* Bevacizumab plus irinotecan, fluorouracil, and leucovorin for metastatic colorectal cancer. *N. Engl. J. Med.* **350**, 2335–2342 (2004).
8. Maxwell, P.H. *et al.* Hypoxia-inducible factor-1 modulates gene expression in solid tumors and influences both angiogenesis and tumor growth. *Proc. Natl. Acad. Sci. USA* **94**, 8104–8109 (1997).
9. Ryan, H.E. *et al.* Hypoxia-inducible factor-1alpha is a positive factor in solid tumor growth. *Cancer Res.* **60**, 4010–4015 (2000).
10. Mizukami, Y. *et al.* Hypoxia-inducible factor-1-independent regulation of vascular endothelial growth factor by hypoxia in colon cancer. *Cancer Res.* **64**, 1765–1772 (2004).
11. Pierce, J.W. *et al.* Novel inhibitors of cytokine-induced IkappaBalpha phosphorylation and endothelial cell adhesion molecule expression show anti-inflammatory effects *in vivo*. *J. Biol. Chem.* **272**, 21096–21103 (1997).
12. Schreck, R., Rieber, P. & Baeuerle, P.A. Reactive oxygen intermediates as apparently widely used messengers in the activation of the NF-kappa B transcription factor and HIV-1. *EMBO J.* **10**, 2247–2258 (1991).
13. Michiels, C., Minet, E., Mottet, D. & Raes, M. Regulation of gene expression by oxygen: NF-kappaB and HIF-1, two extremes. *Free Radic. Biol. Med.* **33**, 1231–1242 (2002).
14. Chandel, N.S. *et al.* Mitochondrial reactive oxygen species trigger hypoxia-induced transcription. *Proc. Natl. Acad. Sci. USA* **95**, 11715–11720 (1998).
15. Chandel, N.S. *et al.* Reactive oxygen species generated at mitochondrial complex III stabilize hypoxia-inducible factor-1alpha during hypoxia: a mechanism of O2 sensing. *J. Biol. Chem.* **275**, 25130–25138 (2000).
16. Brand, K.A. & Hermfisse, U. Aerobic glycolysis by proliferating cells: a protective strategy against reactive oxygen species. *FASEB J.* **11**, 388–395 (1997).
17. Seagroves, T.N. *et al.* Transcription factor HIF-1 is a necessary mediator of the pasteur effect in mammalian cells. *Mol. Cell. Biol.* **21**, 3436–3444 (2001).
18. Sparmann, A. & Bar-Sagi, D. Ras-induced interleukin-8 expression plays a critical role in tumor growth and angiogenesis. *Cancer Cell* **6**, 447–458 (2004).
19. Shirasawa, S., Furuse, M., Yokoyama, N. & Sasazuki, T. Altered growth of human colon cancer cell lines disrupted at activated Ki-ras. *Science* **260**, 85–88 (1993).
20. Ryan, H.E., Lo, J. & Johnson, R.S. HIF-1 alpha is required for solid tumor formation and embryonic vascularization. *EMBO J.* **17**, 3005–3015 (1998).
21. Beasley, N.J. *et al.* Hypoxia-inducible factors HIF-1alpha and HIF-2alpha in head and neck cancer: relationship to tumor biology and treatment outcome in surgically resected patients. *Cancer Res.* **62**, 2493–2497 (2002).
22. Raval, R.R. *et al.* Contrasting properties of hypoxia-inducible factor 1 (HIF-1) and HIF-2 in von Hippel-Lindau-associated renal cell carcinoma. *Mol. Cell. Biol.* **25**, 5675–5686 (2005).
23. Mack, F.A., Patel, J.H., Biju, M.P., Haase, V.H. & Simon, M.C. Decreased growth of Vhl−/− fibrosarcomas is associated with elevated levels of cyclin kinase inhibitors p21 and p27. *Mol. Cell. Biol.* **25**, 4565–4578 (2005).
24. Koshiji, M. & Huang, L.E. Dynamic balancing of the dual nature of HIF-1alpha for cell survival. *Cell Cycle* **3**, 853–854 (2004).
25. Arenberg, D.A. *et al.* Inhibition of interleukin-8 reduces tumorigenesis of human non-small cell lung cancer in SCID mice. *J. Clin. Invest.* **97**, 2792–2802 (1996).
26. Ofori-Darko, E. *et al.* An OmpA-like protein from *Acinetobacter spp.* stimulates gastrin and interleukin-8 promoters. *Infect. Immun.* **68**, 3657–3666 (2000).
27. Khokhlatchev, A. *et al.* Identification of a novel Ras-regulated proapoptotic pathway. *Curr. Biol.* **12**, 253–265 (2002).
28. Zhang, L., Fogg, D.K. & Waisman, D.M. RNA interference-mediated silencing of the S100A10 gene attenuates plasmin generation and invasiveness of Colo 222 colorectal cancer cells. *J. Biol. Chem.* **279**, 2053–2062 (2004).
29. Behre, G., Smith, L.T. & Tenen, D.G. Use of a promoterless Renilla luciferase vector as an internal control plasmid for transient co-transfection assays of Ras-mediated transcription activation. *Biotechniques* **26**, 24–28 (1999).
30. Mohanty, J.G., Jaffe, J.S., Schulman, E.S. & Raible, D.G. A highly sensitive fluorescent micro-assay of H202 release from activated human leukocytes using a dihydroxyphenoxazine derivative. *J. Immunol. Methods* **202**, 133–141 (1997).

CORRIGENDUM: Combating diabetes and obesity in Japan

Y Yazaki & T Kadowaki
Nat. Med. **12**, 73–74 (2006)

In **Box 1**, "(BM ≥125)" should read "(BMI ≥25)."

CORRIGENDUM: ATM regulates target switching to escalating doses of radiation in the intestines

H-J Ch'ang, J G Maj, F Paris, H R Xing, J Zhang, J-P Truman, C Cardon-Cardo, A Haimovitz-Friedman, R Kolesnick & Z Fuchs
Nat. Med. **11**, 484–490 (2005)

In **Figure 2a**, ceramide levels at 8 and 12 h after 16 Gy should have read 102 ± 10 and 118 ± 10 percent of control, respectively, and s.e.m. values for the remaining points should be multiplied by a factor of 2.6.

CORRIGENDUM: Induction of interleukin-8 preserves the angiogenic response in HIF-1α–deficient colon cancer cells

Y Mizukami, W-S Jo, E-M Duerr, M Gala, J Li, X Zhang, M A Zimmer, O Iliopoulos, L R Zukerberg, Y Kohgo, M P Lynch, B R Rueda & D C Chung
Nat. Med. **11**, 992–997 (2005)

In **Figure 3d**, the labels for the cell lines are incorrect. Instead of DLD-1/HIF-wt and DLD-1/HIF-kd, the labels should be Caco2/HIF-wt and Caco2/HIF-kd, respectively.